Ecosystems
https://doi.org/10.1007/s10021-018-0223-7

Vegetation Cover, Tidal Amplitude and Land Area Predict Short-Term Marsh Vulnerability in Coastal Louisiana

Donald R. Schoolmaster Jr.,[1]* Camille L. Stagg,[1] Leigh Anne Sharp,[2] Tommy E. McGinnis,[2] Bernard Wood,[2] and Sarai C. Piazza[1]

[1]*U.S. Geological Survey, Wetland and Aquatic Research Center, 700 Cajundome Blvd, Lafayette, Louisiana 70506, USA;* [2]*Coastal Protection and Restoration Authority of Louisiana, 635 Cajundome Blvd, Lafayette, Louisiana 70506, USA*

Abstract

The loss of coastal marshes is a topic of great concern, because these habitats provide tangible ecosystem services and are at risk from sea-level rise and human activities. In recent years, a significant effort has gone into understanding and modeling the relationships between the biological and physical factors that contribute to marsh stability. Simulation-based process models suggest that marsh stability is the product of a complex feedback between sediment supply, flooding regime and vegetation response, resulting in elevation gains sufficient to match the combination of relative sea-level rise and losses from erosion. However, there have been few direct, empirical tests of these models, because long-term datasets that have captured sufficient numbers of marsh loss events in the context of a rigorous monitoring program are rare. We use a multi-year dataset collected by the Coastwide Reference Monitoring System that includes transitions of monitored vegetation plots to open water to build and test a predictive model of near-term marsh vulnerability. We found that despite the conclusions of previous process models, elevation change had no ability to predict the transition of vegetated marsh to open water. However, we found that the processes that drive elevation change were significant predictors of transitions. Specifically, vegetation cover in prior year, land area in the surrounding 1 km^2 (an estimate of marsh fragmentation) and the interaction of tidal amplitude and position in tidal frame were all significant factors predicting marsh loss. This suggests that (1) elevation change is likely better a predictor of marsh loss at timescales longer than we consider in this study and (2) the significant predictive factors affect marsh vulnerability through pathways other than elevation change, such as resistance to erosion. In addition, we found that, while sensitivity of marsh vulnerability to the predictive factors varied spatially across coastal Louisiana, vegetation cover in prior year was the best single predictor of subsequent loss in most sites followed by changes in percent land and tidal amplitude. The model's predicted land loss rates correlated well with land loss rates derived from satellite data, although agreement was spatially variable. These results indicate (1) monitoring the loss of small-scale vegetation plots can inform patterns of land loss at larger scales, (2) the drivers of

Received 22 September 2017; accepted 2 January 2018

Electronic supplementary material: The online version of this article (https://doi.org/10.1007/s10021-018-0223-7) contains supplementary material, which is available to authorized users.

Authors Contributions DS, CL, LS and SP conceived the ideas; DS, LS, TM and BW designed and carried out the analysis; DS and CL led the writing of the manuscript.

**Corresponding author; e-mail:* schoolmasterd@usgs.gov

Published online: 05 February 2018

land loss vary spatially across coastal Louisiana, and (3) relatively simple models have potential as highly informative tools for bioassessment, directing future research and management planning.

Key words: coastal marsh; stability; monitoring; sea-level rise; erosion; fragmentation; tidal amplitude.

Introduction

Coastal wetlands have long been a focus of intense study, because they provide several tangible ecosystem services and are at risk from sea-level rise and human activities. Globally, the combination of sea-level rise and direct human disruption is predicted to cause the loss of 36–70% of existing wetlands by 2080 (Nicholls and others 1999). Rates of land loss are especially high in coastal Louisiana, which, in addition to experiencing direct human disturbance and reduced sediment supply due to channelization, experiences a high rate of coastal subsidence (Shinkle and Dokka 2007; Glick and others 2013).

Many potential contributing factors to wetland loss, in both coastal Louisiana and more generally, have been identified; however, the relative importance of contributing factors may vary regionally and depend on the spatial and temporal scale considered (Day and others 2008). For example, at the landscape scale, coastal wetlands develop where the rates of accretion and organic soil formation are greater than the rates of erosion, subsidence and sea-level rise, and are maintained where these rates are in equilibrium. These rates are determined at multiple scales by the complex feedback between physical factors, such as frequency and duration of flooding events, and biological factors, such as vegetation biomass production and decomposition rates (Fagherazzi and others 2004; Temmerman and others 2005; Kirwan and Guntenspergen 2010). In numerical models, marsh platform dynamics, and thus marsh stability (that is, resistance to submergence), are driven by flooding, which has the dual effect of increasing the transport of sediments to the marsh surface and stimulating vegetative growth (Morris and others 2002). In turn, vegetation biomass reduces surface-water flow rate and facilitates mineral sedimentation (Leonard and Luther 1995; Ensign and others 2014). Additionally, above- and below-ground biomass contributes to organic soil formation (Nyman and others 1990) and is a significant contributor to accretion (Nyman and others 2006) and elevation change (McKee 2011), all of which feed back onto flood depth and duration (Cahoon and others 2006). These processes interact to drive the absolute elevation change in the marsh, which, when compared with the rate of sea-level rise, determines the relative elevation change ($RSLR_{wet}$, Cahoon 2015), a direct estimate of whether the marsh is on a stable trajectory or losing ground.

One of the main applications of the insights of numerical modeling of coastal marshes has been to use relative elevation change rate as a proxy measure to predict marsh vulnerability. However, it has been difficult to empirically establish how well the putative drivers and measures predict marsh loss of actual coastal wetlands. A major impediment to direct empirical tests of the efficacy of elevation change and accretion as predictive assessment tools for marsh vulnerability is the relative scarcity of appropriate data. There are few datasets with the spatial coverage and temporal duration necessary to test the relationships between physical/biological factors and marsh stability. In this study, we used an 8-year dataset collected by the Coastwide Reference Monitoring System (CRMS) to build a predictive model of marsh vulnerability. These data included measures of vegetation characteristics, marsh elevation, accretion, water level, water temperature and surface-water salinity.

We defined marsh vulnerability as the probability of transition from vegetated marsh to open water and used the CRMS dataset to identify transition events of monitored vegetation plots to open water. We selected this measure of marsh vulnerability, because it can include both shoreline losses to erosion and interior losses to subsidence. Furthermore, the spatial and temporal scale of these transition events provides a robust dataset to support quantitative analysis.

The goal of these analyses was to combine current theory of marsh vulnerability with data from the CRMS program to develop a predictive model of marsh loss that can be applied to coastal wetlands to identify areas at greatest risk of marsh loss, inform distribution of management resources and evaluate restoration project effectiveness. To this end, we used results from the literature to develop a statistical model of marsh vulnerability that could be tested with data from the CRMS program. We found, despite wide theoretical support, RSET-measured elevation change had no ability to pre-

dict transition events in the subsequent year. Based on the results of that analysis, we derived and fit an alternative model that included the hypothesized drivers of elevation change to predict transition events and used multiple methods to rigorously assess the model's goodness of fit. Finally, we validated the predictive model by comparing its predictions to independent data: historical rates of land loss quantified with Landsat-TM data by Couvillion and others (2011).

Methods

Model Description

The stability of coastal marshes depends on both vertical and horizontal processes: elevation change rates that keep pace with rates of relative sea-level rise and resistance to erosion at the marsh–water interface (Mariotti and Carr 2014; Kirwan and others 2016). Multiple processes interact through hydrogeomorphic feedbacks to influence wetland elevation gains (Cahoon and others 2006). For example, tidal deposition of mineral sediments can stimulate vegetation production (Harrison and Bloom 1977; Friedrichs and Perry 2001), which, in turn, contributes to elevation gains directly through root zone expansion (McKee 2011) and indirectly through enhancing mineral sediment and organic matter accretion (Ensign and others 2014). Furthermore, as tidal amplitude increases, primary production increases at lower elevations resulting in increased sediment deposition and subsequently, increased resistance to loss (Kirwan and Guntenspergen 2010; Supplemental Appendix). At the marsh–water interface, lateral erosion increases with both the power of incident waves and the total length of exposed marsh margin (Mariotti and Fagherazzi 2010; Marani and others 2011). As such, an increase in the length of exposed marsh margin, such as would occur with fragmentation, is associated with greater risk of loss to erosion and thus increased vulnerability to land loss (Couvillion and others 2016).

To account for the major processes associated with marsh stability, we derived an initial model that included RSET-measured elevation change and a proxy measure of land fragmentation. While we have direct measures of elevation change, we do not have direct measures of land fragmentation. As a proxy, we used the percent land in the surrounding square-kilometer of each site as a measure of land fragmentation.

In an alternative model, we replaced measured elevation change with variables representing its hypothesized drivers, as well as other factors thought to drive marsh stability. In this model, we included measures of vegetation production, tidal range and position in the tidal frame. We detail the rationale for each of these measures below.

Production of vegetation biomass is a critical ecosystem function in coastal marshes that contributes to marsh stability through multiple pathways. Energetically, macrophytes are the most abundant primary producers in the marsh (Teal 1962) and play a key role in regulating stability. For example, Turner and others (2004) found that marshes with greater belowground biomass recovered more quickly from disturbances than marshes with lower energy reserves in the belowground biomass pool. In addition to providing the basis for all energy flow in the marsh, macrophyte primary production is a key process driving hydrogeomorphic feedbacks among sediment accretion, elevation change and flooding (Morris and others 2002; Mudd and others 2009; Baustian and others 2012). Ideally, these feedbacks maintain the relative elevation of the marsh within the tidal frame and promote persistence of the marsh during periods of sea-level rise (Cahoon and others 2006; Kirwan and Guntenspergen 2012). However, marsh resilience to sea-level rise is compromised when feedbacks between flooding and vegetation growth are disrupted (Marani and others 2007). Following disturbances where vegetation is removed, these hydrogeomorphic feedbacks break down, and marshes and mangroves often convert to unvegetated mudflats (Cahoon and others 2003; Kirwan and Murray 2008). We used percent cover as an estimate of vegetative production.

Tidal range and position in the tidal frame are hypothesized to have an interactive effect on marsh stability. Wetlands high in the tidal frame are hypothesized to benefit from having a 'head-start' on SLR or elevation capital (Cahoon 2015). However, areas lower in the tidal frame benefit from deeper flooding, which is a key factor that regulates marsh stability through enhancing sediment accretion and biomass production. As flooding increases, opportunity for the deposition of suspended sediment increases (Friedrichs and Perry 2001). Increasing tidal range is hypothesized to promote equilibrium lower in tidal frame (Kirwan and Guntenspergen 2010) due to increased primary production at lower elevations. The increased biomass promotes sediment deposition (Ensign and others 2014) via reduced flow velocity (Leonard and Luther 1995; van de Koppel and others 2005), and the net result of increasing tidal range is greater resistance of the marsh to perturbations. (A de-

tailed derivation of this result is presented in Supplemental Appendix.) In contrast, the benefit of higher position in the tidal frame is reduced with increasing tidal range. In the alternative model, we included tidal amplitude as a measure of tidal range and daily average depth of flooding events as an estimate of position in the tidal frame.

Data Description

CRMS Sites

In 2004, the Coastwide Reference Monitoring System-Wetlands (CRMS) was implemented by the Coastal Wetland Planning, Protection, and Restoration Act (CWPPRA) to provide a network of reference sites to assess restoration activities (Steyer and others 2003). The 392 CRMS sites were randomly selected from approximately 7000 potential coastal wetland sites using a stratified random design (Steyer and others 2003) where sites were allocated to major coastal wetland types (fresh, intermediate, brackish, saline and swamp) according to distributions of those habitats (Visser and Sasser 1998). For this study, all swamp sites and floating marsh sites were removed from the analysis, leaving 290 sites.

Each CRMS site includes stations used for measuring surface elevation change and vertical accretion, a hydrology station for measuring hourly water elevation and salinity and a 282.8-m transect where vegetation community data are collected.

RSET Data

Rod surface elevation table (RSET) methods (Cahoon and others 2002) were used to measure small changes in elevation within CRMS sites. One RSET benchmark is located at each CRMS site where it is possible to measure an attached soil surface. Sites were measured in 6-month intervals to provide an estimate of cumulative elevation change over time. Details of the RSET measurement methodology as implemented in CRMS are available in Folse and others (2014). For each sampling event, mean elevation was calculated for each of four cardinal directions, and elevation change was calculated for each site using a linear regression of cumulative elevation change versus time from 2008 to 2015.

Vegetation Data

Vegetation sampling was conducted within ten 2 m $\times$ 2 m vegetation stations along the vegetation transect at each CRMS site (Cretini and others 2011; Folse and others 2014). Stations were sampled annually. At each station, the percent cover of each plant species was visually estimated at the peak of growing season (July 15–August 31). For this study we used total cover as an indicator of plant productivity. A complete description of the methods and sampling design for collecting vegetation data in emergent marsh can be found in Folse and others (2014).

In addition to using vegetation cover as a predictor variable of marsh vulnerability, as described above, we also used plant cover to identify transition events. A transition from marsh to open water was identified when: (1) a site had a nonzero value for total cover at the beginning of the sample interval (that is, 2007) and (2) at some point in the interval (2007–2014) a zero value for total cover was recorded and (3) total cover values remained below 5% for the station for all subsequent years. The year at which the first zero value for cover was recorded as the year the transition occurred. To translate these into a vector of binary responses indicating transition events, years with nonzero values for cover were recorded as zero (that is, no transition to open water occurred), a one was recorded for the year the transition took place, and all years subsequent to the transition event were recorded as 'NA' to indicate missing data. As a predictor variable, we used mean total cover across all stations in each site in the preceding year (year $(t-1)$).

Hydrologic Data

Tidal amplitude was calculated from hydrologic data that are collected hourly at all CRMS sites. Water level, temperature, specific conductivity and salinity data are collected hourly from surface water at permanent monitoring stations. The water-level benchmark was surveyed using real-time kinematic technology, and water levels are referenced to the NAVD 88 datum (Folse and others 2014). The calculation of mean tidal amplitude from hourly data followed the harmonic tidal analysis methods described in Snedden and Swenson (2012) using data from 2008 to 2014.

Land/Water Data

Percent land was calculated from a land/water classification analysis based on data from digital imagery captured with at 1-m resolution with Digital Mapping Camera (DMC) in 2012. Leica imaging software was used to perform an unsupervised classification based on the range of pixel values into one of 50 classes. These classes were recoded into one of three categories: land, water and flooded land. For this analysis, we combined the

land and flooded land categories within the 1 km^2 area surrounding each CRMS site and converted it to percent land.

Vulnerability Analysis

The response variable for this model is the probability of at least one transition event in site j in year t, $P(y_{jt} = 1)$. The potential predictor variables vary in one of two ways, across sites but not years (x_j) (that is, percent land) or across sites and years (x_{jt}) (that is, elevation change, vegetation cover, flood depth and tidal amplitude). This gives the model,

$$P(y_{jt} = 1) = \log it^{-1}(\beta 0 + \beta 1 X 1_{jt-1} + \beta 2 X 2_j)$$

where y_{jt} indicates a transition event at any station in site j at time t, $\beta 0$ is a site-level intercept, $\beta 1$ are slopes of time-varying predictors, and $\beta 2$ are slopes of constant site-level predictors. This model assumes that the probability of a transition to open water at a given station at time t is independent of the probability of a transition to open water at the same station at time $t - 1$, given the set of predictors and that transition has not yet happened, that is,

$$P(y_{ijt} = 1) \perp\!\!\!\perp P(y_{ijt-1} = 1) | X, y_{ijt-1} \neq 1.$$

We fit the model using a generalized linear model with a binomial distribution and logit link function. This was done with the glm function in the stats package on the R statistical platform (R Core Team 2015). We tested the assumption of temporal independence by examining the lag-1 temporal autocorrelations of the Pearson residuals within sites.To estimate the relative effect of each factor on the probability of transition, we calculated the local sensitivity of each significant predictor for each CRMS site as

$$\phi_{ij} = \frac{\partial \hat{P}(y_j = 1)}{\partial x_{ij}} x_{ij}|_{\beta, \bar{X}_j}$$

where $\hat{P}(y_j = 1)$ is the predicted probability of a transition event in site j, β is the vector of parameters of the model, and $\bar{X}_j$ is the matrix of time-averaged values of the drivers in site j. The output of this gives, for each site, the percent change in the probability of transition given a 1% increase in value of driver i in site j.

Missing Data

Fewer and 3% of values were missing for cover (2.3%), flood depth (2.9%) and percent land (1.7%). Percent of missing data for tidal amplitude and elevation change were 5.1% and 14.4%, respectively. Missing data were imputed using a multiple imputation procedure implemented by the amelia() function from the Amelia package (Honaker and others 2011). The final estimates for missing values used for analysis were derived by replacing each missing value with the median of its corresponding values across all imputed datasets. We assessed the efficacy of this method testing the null hypothesis that the estimates generated using the median values for the missing data across 100 imputed datasets were sampled from the distribution of estimates generated by fitting each imputation separately. We failed to reject the hypothesis for each variable (cover $p = 0.92$; tidal amplitude $p = 0.13$; flood depth $p = 0.19$; percent land $p = 0.78$; tidal amplitude $\times$ flood depth $p = 0.17$).

Model Validation

In addition to the standard model validation metrics typically calculated for logistic regressions, such as AUC, true-positive and true-negative rates, we conducted predictive checks for the fitted model (Gelman and Hill 2009). To do this we used the fitted parameters to simulate 1000 datasets of similar form to the observed data and used these to construct visualizations to evaluate the ability of the fitted model to reproduce the patterns observed in the original data. We used the model-simulated data to predict the number of sites experiencing at least one transition event for each year and the number of years each site experienced at least one transition event.

To test the classification accuracy of the model, we calculated the 'cutoff value' of the predicted probabilities that maximized the correct classification rate and then used that cutoff rate to calculate the optimum classification table for each model (Hosmer and Lemeshow 2000).

Comparison with Historical Land Loss Rates

To assess the model's accuracy at site and basin-wide spatial scales, we compared the predictions of the fitted model to historical annual land loss rates estimated from Landsat-TM based data from 1985 to 2010 (Couvillion and others 2011). These data included estimates of land area for each CRMS site. We estimated an annual loss rate, r_{obs}, as the slope of the relationship between log(Land Area) and time, where 1985 was used as the reference date (that is, $t = 0$). Because we wanted to compare

these to loss rates derived from probabilities of land loss estimated from the logistic regression model, any sites that experienced net land gain (that is, $r_{obs} < 0$) were set to zero.

The average annual probability of land loss in site j was estimated from the model as

$$r_j = 1 - \left(\prod_{t=1}^{T} 1 - \hat{P}(y_{jt} = 1) \right)^{\frac{1}{T}},$$

where $\hat{P}(y_{jt} = 1)$ is the predicted probability of a transition event in site j in year t, and T is the total number of years for which predictions were calculated.

Results

Model Selection and Validation

The initial model, which included RSET-measured elevation change and percent land as predictors, fit the data much better than a null model which included only an intercept term ($\Delta AIC = 40.1$). However, elevation change did not improve the fit compared to a model that used only percent land ($\Delta AIC = 1.82$) (Figure 1).

The alternative model, which replaced the direct measurement of elevation change with tidal amplitude, flood depth and vegetation cover, fit the data much better than the null, intercept-only model ($\Delta AIC = 78.83$) and better than the initial model ($\Delta AIC = 40.56$). The parameter estimates of the alternative model are shown in Table 1. The temporal correlation of the Pearson residuals was small ($r = -0.05$, $p = 0.579$), suggesting that temporal nonindependence had little influence on the model estimates.

The alternative model distinguishes well between sites that experienced a transition and those that did not. The mean predicted probability of transition for sites that actually experienced a transition event in a given year was 0.075, whereas the predicted probabilities for sites that did not was 0.005 ($t = -9.62$, $df = 33.31$, p value $\ll 0.01$, AUC = 0.882). The cutoff predicted probability that optimally separated the groups was 0.02, resulting in a true-positive rate of 81.8% and a true-negative rate of 83.8%.

The predictive checks of this model show that across all sites, the model predicts well the number of transition events for all years (Figure 2B). For each year, the observed number of events falls within the 95% confidence interval predicted by the model. The model does show some variation in the ability to correctly predict the total number of

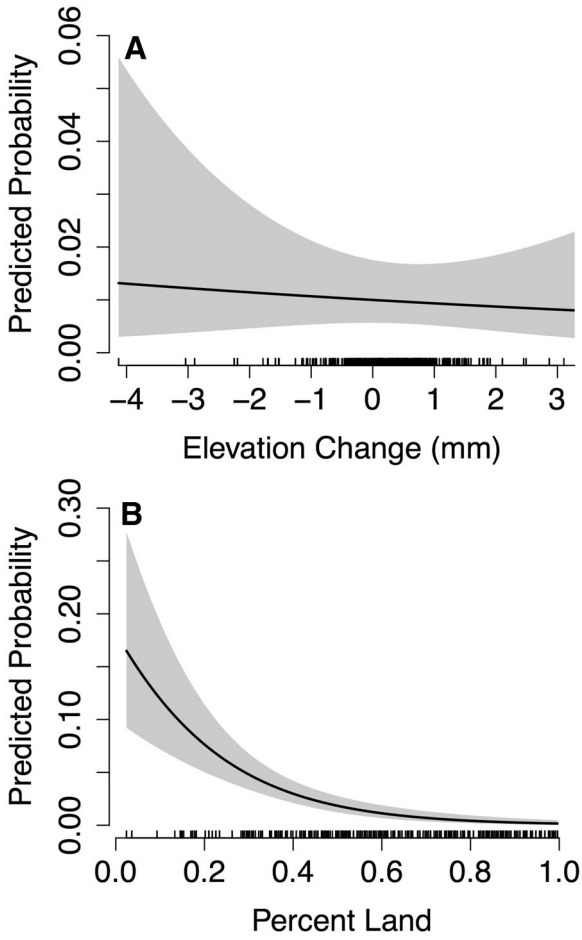

Figure 1. Relationships between predictor variables and model-predicted probability of transition for the initial model for **A** RSET-measured elevation change and **B** percent land. The gray envelope indicated 95% confidence region. The hashes on the x-axis indicate observed data for that variable.

events per site. Figure 2A shows for most sites that experienced at least one transition event, the model predicts well the number of years that it will experience at least one event (that is, the observed number of events falls within the 95% confidence interval predicted by the model). In one site, the actual number of years with at least one transition event falls outside the bounds predicted by 1000 simulations of the model. In site CRMS2166, the model under-predicted the number of events (0 predicted vs. 1 observed), suggesting that the model is potentially missing a factor associated with vulnerability that is present at this site. There are three sites in which the observed number of transition events fell below the median number predicted by the model. These sites represent potential 'bright spots,' that is, they are more stable than predicted by the model (Cinner and others 2017). For site

Table 1. Estimated Parameters for Logistic Regression Model

	Estimates	Std. error	*P* value
Intercept	1.03	0.82	0.211
Cover	− 4.59	0.91	< 0.001
%Land	− 5.87	0.91	< 0.001
Tidal Amp.	0.17	0.07	0.009
Flood Depth	0.08	0.03	< 0.001
Tidal Amp. × Flood Depth	− 0.01	0.004	0.002

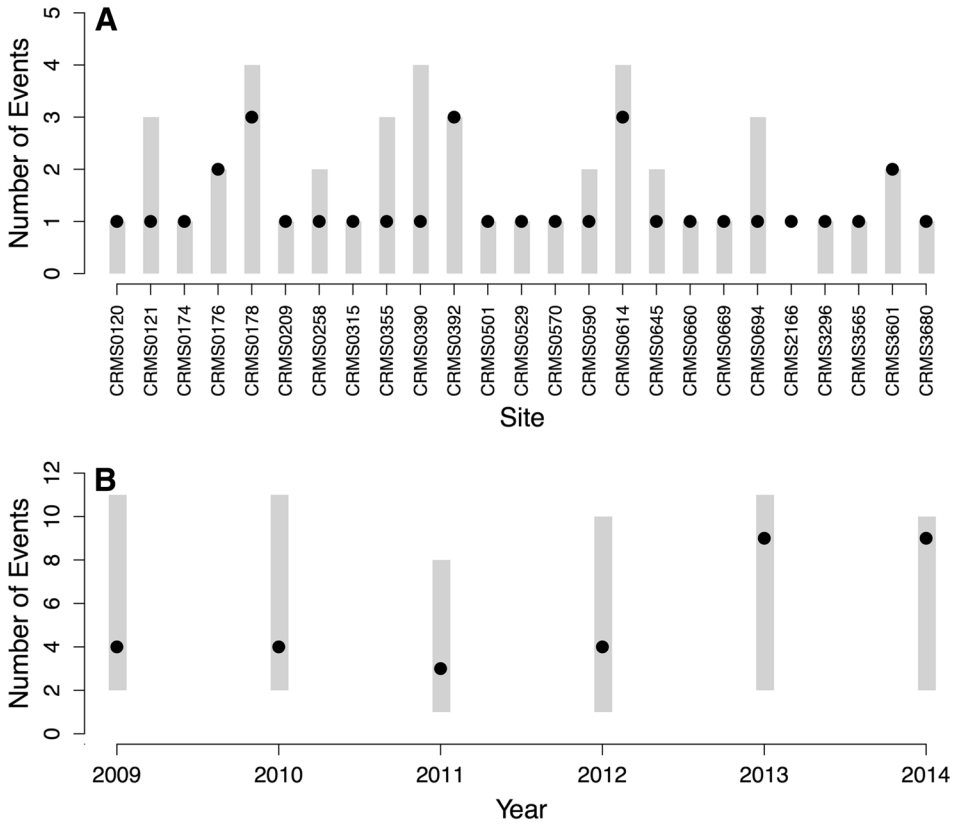

Figure 2. Posterior predictive checks of fitted model. In **A** the gray rectangles show the 95% confidence interval of number of predicted transition events in each site that experienced at least one event for all years over 1000 simulations of the model. The maximum possible number of transition events per site is 10. The black circles show the observed number of transition events in each site across all years. The gray rectangles in **B** show the 95% confidence interval for the predicted number of transition events per year over all sites from 1000 simulations of the model. Black circles show the observed number of transition events per year.

CRMS0390, the median number of years predicted to have at least one transition event was two; only 1 was observed. The median number of years with events for sites CRMS0567 and CRMS2418 was one; none were observed.

Parameter Interpretation

Interpreting the estimated parameters is difficult given logit transformation; however, the sign of the estimate is informative. Positive values of estimated parameters indicate that increased values of the predictor are associated with an increased probability of transition to open water (that is, greater vulnerability, lesser stability). Negative parameter estimates indicate that larger predictor values are associated with lower probability of transition (that is, lesser vulnerability, greater stability). Thus, the model suggests that those sites that are less fragmented and have more vegetation cover are more stable than sites that are more fragmented, and have less cover (Figure 3).

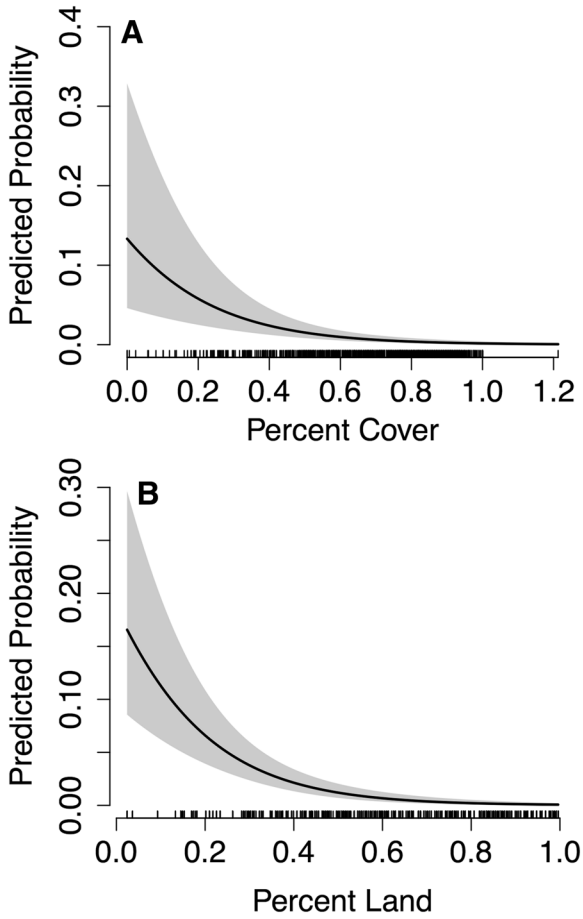

Figure 3. Relationships between predictor variables and model-predicted probability of transition for the alternative model for **A** percent cover in previous year and **B** percent land. The gray envelope indicated 95% confidence region. The hashes on the x-axis indicate observed data for that variable.

Due to the interaction between tidal amplitude and flood depth, the relationship with marsh stability is complex. We hypothesized that the benefit of being higher in the tidal frame was mediated by larger tidal range. This hypothesized relationship was observed in the data and is represented by the negative parameter associated with the interaction of tidal amplitude and flood depth. Given small tidal amplitudes, higher daily flood depth (that is, lower position in the tidal frame) is associated with an increased probability of transition (Figure 4A). However, given a larger tidal amplitude, the benefit of greater daily flood depth out-weighs the risks, resulting in a lower probability of transition (greater stability) (Figure 4B, C).

To compare the importance of each predictor and how it may change over the coast, we calculated local sensitivities of each predictor at each site.

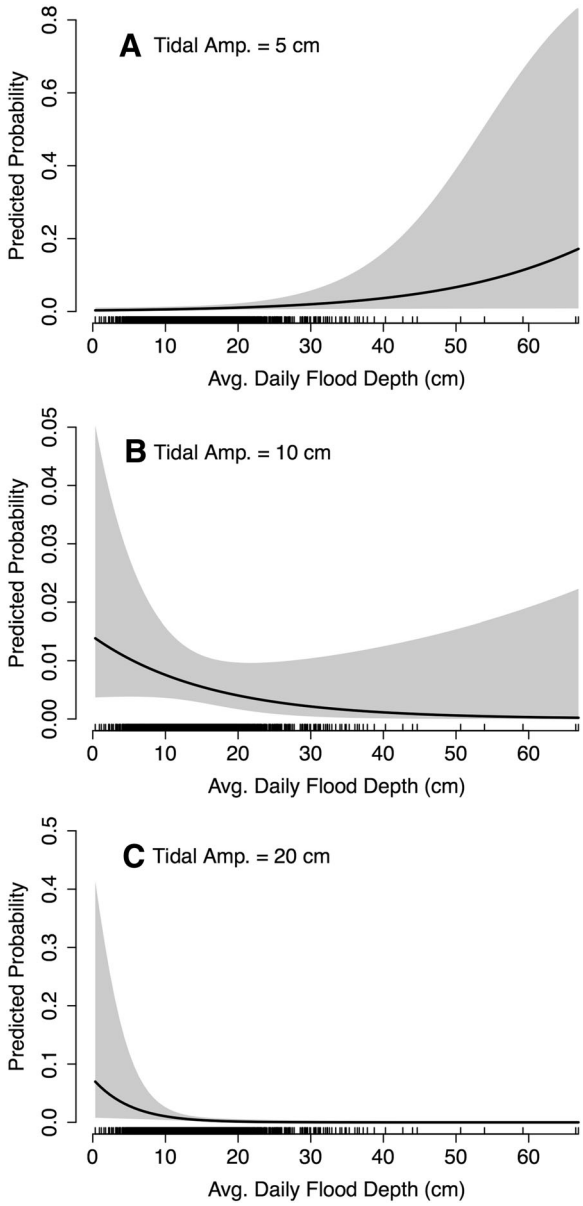

Figure 4. Relationships between average daily flood depth (an indicator of position in tidal frame) and model-predicted probability of transition at different tidal amplitudes. **A** At very low tidal amplitude (5 cm) increasing average daily flood depth increases marsh vulnerability. At larger tidal amplitudes (for example, **B** 10 cm and **C** 20 cm) increasing flood depth is associated with an increased marsh stability. The gray envelope indicated 95% confidence region. The hashes on the x-axis indicate observed data for that variable.

Figure 5 shows how the sensitivities vary across the nine hydrologic basins of the Louisiana coast (described in CWPPRA 1993). It shows that six of the nine hydrologic basins were most sensitive to changes in vegetative cover. Two basins, Mermentau and Teche/Vermilion, were most sensitive

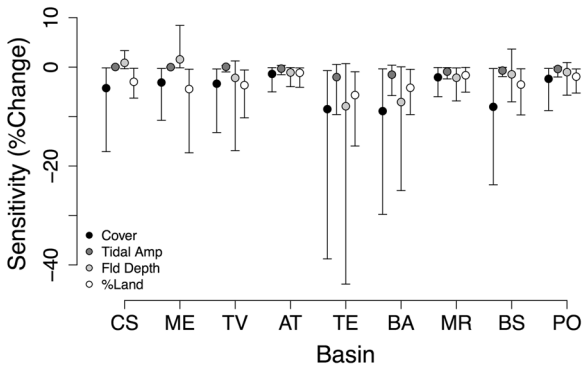

Figure 5. Scaled local sensitivity of predicted probability of transition to each of the model's predictors across the nine hydrologic basins of Coastal Louisiana. Basins are arranged west to east with the following abbreviations: CS—Calcasieu/Sabine, ME—Mermentau, TV—Teche/Vermilion, AT—Atchafalaya, TE—Terrebonne, BA—Barataria, MR—Mississippi River, BS—Breton Sound, PO—Pontchartrain. The scaled sensitivity is the percent change in predicted probability of transition given a one percent change in the predictor.

to changes in percent land, and one, Mississippi River, was most sensitive to flood depth. The effect of the interactive nature of tidal amplitude and flood depth is displayed in Figure 5. In the westernmost basins, where tidal amplitude is very small (< 2 cm), vulnerability increased with small changes in flood depth (that is, sensitivity > 0). In contrast, in the central basins, where tidal amplitude is higher (> 15 cm), increases in flood depth (that is, lower position in tidal frame) are associated with increasing stability. As evidenced by the length of the error bars, the sensitivity analysis also shows that some basins are much more heterogeneous than others, in the sense that the sensitivity to the drivers varies more across sites in some basins, such as Terrebonne and Barataria, than others, such as Atchafalaya and Mississippi River.

Comparison with Historical Land Loss Rates

The correlation between model predictions and historical loss rates derived from satellite data across all sites is high ($r = 0.622$, $p < 0.01$) (Figure 6). Moreover, the predicted and observed loss rates tend to fall along the 1:1 line, indicating that the model predicts the actual loss rates well. The correspondence between predicted and historical loss rates varies across the hydrologic basins (Figure 6). Although the model predicts the observed average loss rates of each basin well ($r > 0.4$), the basins east of the Atchafalaya Basin are, with the exception of the Pontchartrain Basin, predicted much better ($r > 0.68$) than those to the west. This pattern suggests the existence of variation in the processes contributing to land loss between the eastern and western basins.

Discussion

We used long-term monitoring data from coastal Louisiana to test predictors of marsh transition to open water. We found that elevation change was not a significant predictor of transition events in the subsequent year. Instead, we found that vegetation cover, tidal amplitude, position in tidal frame and the relative amount of land in the surrounding area were significant predictors of marsh vulnerability. The reason that elevation change did not predict land loss events is likely due to differences in temporal scale between the measure of elevation change and the transition event. The response variable we used was the probability of at least one transition event in the site in the subsequent year, a near-term prediction. Because elevation change is thought to be an important indicator of the marsh's ability to track sea-level rise, a long-term assessment, it might not be surprising that elevation change in one year is not predictive of the probability of land loss in the next year. It seems likely, therefore, that we would have found greater predictive ability of elevation change had we used a longer-term rates of land loss.

Each of the predictors in the final model was chosen based on theorized relationships with marsh stability. It is likely that the predictive signal of near-term land loss demonstrated by the variables is derived from relationships with drivers of both long-term and near-term stability, such as elevation change and resistance to erosion, respectively. For example, in addition to increasing sedimentation rate, vegetation can also function to attenuate wave energy (Gedan and others 2011) and modify soil to resist erosion (Feagin and others 2009). Similarly, in addition to the effect of tidal range on stability described by Kirwan and Guntenspergen (2010) and in Supplemental Appendix, tidal range may increase resistance to erosion by distributing wave energy over a greater distance of the tidal cycle (Rosen 1977).

The predictive variable most directly related to erosional resistance was the relative amount of land (versus water) in the surrounding area. It is a measure correlated with both the length of exposed marsh margin and/or the fragmentation of the marsh landscape. Our model predicted that marshes with less fragmentation were also less vul-

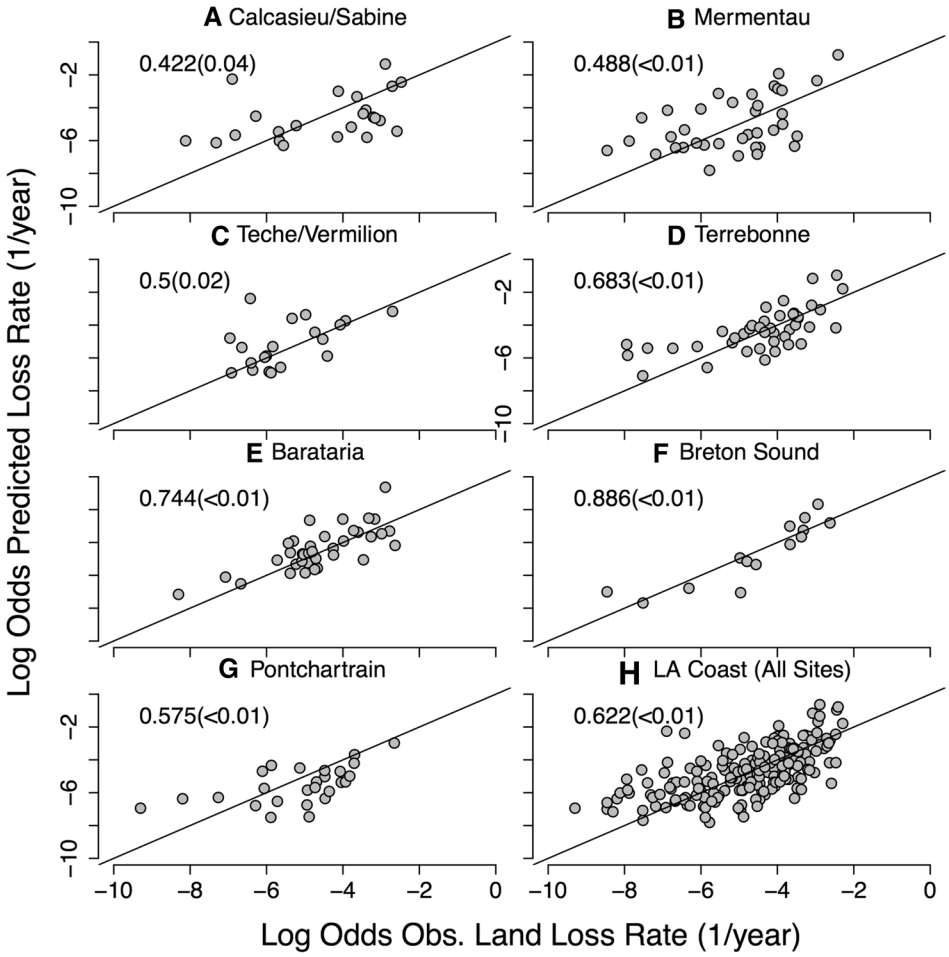

Figure 6. Comparison of model-derived and Landsat-TM-derived historical loss rates at CRMS sites within the 7 hydrologic basins **A**–**G** that had enough data to support statistical conclusions and **F** all sites combined. The legend in each subplot shows the correlation coefficient and *p* value (in parentheses) for the relationship in that basin. The lines in each plot are identity lines showing 1:1 relationship.

nerable to collapse, which is supported by recent spatial analyses of coastal Louisiana (Couvillion and others 2016). In this model, we used land area estimates from a single year (2012). Although we believe that the model would be improved with annual estimates, the strong effects of land area that we observed suggest that the pattern of variation in land area across sites remained similar over the timescale of these data. Previous analyses have associated the spatial patterns of marsh loss with specific mechanisms of land loss. For example, submergence, which occurs as a result of subsidence, generally occurs in the interior marsh, beginning with the formation of small ponds that eventually coalesce and convert to large areas of open water (DeLaune and others 1994; Friedrichs and Perry 2001; Hartig and others 2002). The mechanism of this effect is likely associated with how fragmentation alters the flow of water into and out of the marsh, and thus modifies where and whether deposition of sediment occurs (Bass and Turner 1997). Therefore, the organization of the landscape structure can indicate the mechanisms of loss, inform historic trends and future trajectories of marsh loss (Kennish 2001) and also serve as an indicator for vulnerability (Couvillion and others 2016).

The alternative predictive model performed well in model validation assessments. It showed high levels of sensitivity and specificity as measured by the true-positive and true-negative rates. Furthermore, posterior predictive validation via simulation showed that the model was able to predict the number of years with at least one transition event in most sites and total number of sites with at least one transition event per year in the observed data, indicating the model is well specified.

However, the strongest test for any predictive model is how well it predicts patterns from independent data (that is, data from a source other than that used to calibrate/train the model). We converted the predictions of this model to an average annual probability of land loss to be compared with average annual land loss rates calculated from Landsat-TM data. We found that predictions from a model based on transitions of annually resampled vegetation plots were highly correlated with the land loss rates estimated using satellite data (Figure 6). The variation in predictive ability of the model across the hydrologic basins of coastal Louisiana suggests variation in the drivers of land loss. For example, the existence of areas where satellite-derived land loss rates are less well predicted, suggests spatial variation in parameters associated with the drivers included in the model or the existence of additional, unidentified drivers. However, the overall ability of the model to predict land loss more generally illustrates the effectiveness of using transition events in monitoring sites as an indicator of larger-scale land loss.

A predictive model, such as this, that links local measurements with probability of larger-scale land loss can be an important tool for management and restoration planning. The model suggests some causal drivers of marsh vulnerability and, therefore, can be used to identify mitigation and restoration strategies specifically targeted for those drivers. Moreover, the model can be used to identify where loss is likely to occur in the near future, which could help managers to develop more effective restoration/mitigation strategies, spatially and temporally.

Used as a tool to guide further inquiry, important information can be derived from sites where the model fit is weak. For example, comparing the observed number of transition events to the distribution predicted by simulation of the fitted model allows for the identification of 'bright spots' and 'dark spots,' that is, sites that are more stable or less stable than predicted by the model. Analyses of these sites could help identify additional drivers of stability (Cinner and others 2017). At the basin scale, Figure 6 shows that this model predicts historic land loss rate better in the central and eastern hydrologic basins of Louisiana than in the westernmost basins. This suggests either variation in the identity of drivers or variation in the estimated coefficients between these areas. Finally, the analysis showed that sensitivity of marsh vulnerability to the predictors varied both within and across basins. This information can be used to inform the efficacy of different potential restoration activities (for example, targeting vegetation production vs. tidal reconnection) in different areas across the Louisiana coast.

Finally, although this study included only coastal marshes of Louisiana, we expect the identity of predictors, if not the exact parameter estimates to be generalizable to other coastal wetlands. We developed our statistical models from general theory, as opposed to taking a data mining approach, which would result in more specific, but less interpretable models. The high degree of out-of-sample predictive ability achieved by this confirmatory framework allows an increased confidence in the generality of these results and reflects favorably on the current state of theory of coastal marsh stability.

Conclusion

We have shown that a predictive model of marsh stability estimated from a long-term monitoring data can be used to test our current understanding of drivers of marsh stability. The model confirms that quantitatively assessing marsh vulnerability requires including indicators of its ability to respond dynamically to rising sea level, such as vegetation cover, tidal amplitude and position in the tidal frame, as well as indicators of the its landscape-level context, such as degree of fragmentation or exposure to wave energy. Finally, we have shown that output from site-level models can be scaled up to inform basin or coast-wide assessment tools. These models correlated well with independent historical measures of land loss and thus can be used for predicting land loss, directing management resources and estimating effects of large-scale restoration projects.

Data Availability

The CRMS data are available for public download at the Web site of the Coastal Protection and Restoration Authority: https://cims.coastal.louisiana.gov/monitoring-data/ and at the Web site of the Coastal Wetlands Planning, Protection and Restoration Act: https://www.lacoast.gov/crms2/home.aspx.

Acknowledgements

This work was supported by the CRMS Program, which is administered by CPRA and USGS and is funded through Coastal Wetland Planning Protection and Restoration Area, the State of Louisiana, with federal resource agencies including USFWS,

NMFS, NRCS, EPA and the USACOE. Any use of trade, firm or product names is for descriptive purposes only and does not imply endorsement by the U.S. Government.

FUNDING

This work was supported by the CRMS Program, which is funded through the Coastal Wetlands Planning, Protection, and Restoration Act and the State of Louisiana. A task force of federal agencies, representing USACOE, USFWS, NOAA, NRCS and EPA, governs CWPPRA and provides oversight to CPRA and USGS for the implementation of CRMS.

Compliance with Ethical Standards

Conflict of interest The authors declare that they have no conflict of interest.

REFERENCES

Bass A, Turner RE. 1997. Relationships between salt marsh loss and dredged canals in three south Louisiana estuaries. J Coas Res 13:895–903.

Baustian JJ, Mendelssohn IA, Hester MW. 2012. Vegetation's importance in regulating surface elevation in a coastal salt marsh facing elevated rates of sea level rise. Global Change Biol 18:3377–82.

Cahoon DR. 2015. Estimating relative sea-level rise and submergence potential at a coastal wetland. Estuar Coasts 38(1077):1084.

Cahoon DR, Lynch JC, Perez BC, Segura B, Holland RD, Stelly C, Stephenson G, Hensel P. 2002. High precision measurement of wetland sediment elevation—II. The rod surface elevation table. J Sedim Res 72:734–9.

Cahoon DR, Hensel P, Rybczyk J, McKee KL, Proffitt CE, Perez BC. 2003. Mass tree mortality leads to mangrove peat collapse at Bay Islands, Honduras after Hurricane Mitch. J Ecol 91:1093–105.

Cahoon DR, Hensel PE, Spencer T, Reed D, McKee KL, Saintilan N. 2006. Coastal wetland vulnerability to relative sea-level rise: wetland elevation trends and process controls. In: Verhoeven JTA, Beltman B, Bobbink R, Whigham DF, Eds. Wetland and natural resource management. Berlin: Springer. p 271–92.

Cinner JE et al. 2017. Bright spots among the world's coral reefs. Nature 535:415–19.

Coastal Wetlands Planning, Protection and Restoration Act (CWPPRA). 1993. Louisiana coastal wetlands restoration plan. CWPPRA Program Reports.

Couvillion BR, Barras JA, Steyer GD, Sleavin W, Fischer M, Beck H, Trahan N, Griffin B, Heckman D. 2011. Land area change in coastal Louisiana from 1932 to 2010. U.S. Geological Survey Scientific Investigations Map 3164, Scale 1:265,000, pamphlet.

Couvillion BR, Fischer MR, Beck HJ, Sleavin WJ. 2016. Spatial configuration trends in coastal Louisiana from 1985 to 2010. Wetlands 36:347–59.

Cretini KF, Visser JM, Krauss KW, Steyer GD. 2011. CRMS vegetation analytical team framework—methods for collection, development, and use of vegetation response variables. U.S. Geological Survey Open-File Report 2011–1097.

Day JW, Christian RR, Boesch DM, Yanez-Arancibia A, Morris J, Tilley RR, Naylor L, Schaffner L, Stevenson C. 2008. Consequences of climate change on the ecogeomorphology of coastal wetlands. Estuar Coasts 31:477–91.

DeLaune RD, Nyman JA, Patrick WH Jr. 1994. Peat collapse, ponding and wetland Loss in a rapidly submerging coastal marsh. J Coast Res 10:1021–30.

Ensign SH, Hupp CR, Noe GB, Krauss KW, Stagg CL. 2014. Sediment accretion in tidal freshwater forests and oligohaline marshes of the Waccamaw and Savannah Rivers, USA. Estuar Coasts 37:1107–19.

Fagherazzi S, Marani M, Blum LK. 2004. Introduction: the coupled evolution of geomorphological and ecosystem structures in salt marshes. In: Fagherazzi S, Marani M, Blum LK, Eds. The ecogeomorphology of tidal marshes, coastal Estuarine Stud. Washington, DC: AGU. p 1–5.

Feagin RA, Lozada-Bernard SM, Ravens TM, Möller I, Yeager KM, Baird AH. 2009. Does vegetation prevent wave erosion of salt marsh edges? PNAS 106:10109–13.

Folse TM, Sharp LA, West JL, Hymel MK, Troutman JP, McGinnis TE, Weifenbach D, Boshart WM, Rodrigue LB, Wood WB, Miller CM. 2014. A standard operating procedures manual for the coastwide reference monitoring system-wetlands: methods for site establishment, data collection, and quality assurance/quality control. Baton Rouge, LA: Louisiana Coastal Protection and Restoration Authority. p 228.

Friedrichs CT, Perry JE. 2001. Salt marsh morphodynamics: a synthesis. J Coast Res 27:7–37.

Gedan KB, Kirwan ML, Wolanski E, Barbier EB, Silliman BR. 2011. The present and future role of coastal wetland vegetation in protecting shorelines: answering recent challenges to the paradigm. Clim Change 106:7–29.

Gelman G, Hill J. 2009. Data analysis using regression and multivariate/hierarchical models. New York, NY: Cambridge University Press.

Glick P, Clough J, Polaczyk A, Couvillion B, Nunley B. 2013. Potential effects of sea-level rise on coastal wetland in Southeastern Louisiana. J Coast Res 63:211–33.

Harrison EZ, Bloom AL. 1977. Sedimentation rates on tidal salt marshes in Connecticut. J Sediment Petrol 47:1484–90.

Hartig EK, Gornitz V, Kolker A, Mushacke F, Fallon D. 2002. Anthropogenic and climate-change impacts on salt marshes of Jamaica Bay, New York City. Wetlands 22:71–89.

Honaker J, King G, Blackwell M. 2011. Amelia II: a program for missing data. J Stat Softw 45:1–47.

Hosmer DW Jr, Lemeshow S. 2000. Applied logistic regression. New York: Wiley.

Kennish M. 2001. Coastal salt marsh systems in the U.S.: a review of anthropogenic impacts. J Coast Res 17:731–48.

Kirwan ML, Guntenspergen GR. 2010. Influence of tidal range on the stability of coastal marshland. J Geophys Res 115:F02009.

Kirwan ML, Guntenspergen GR. 2012. Feedbacks between inundation, root production, and shoot growth in a rapidly submerging brackish marsh. J Ecol 100:764–70.

Kirwan ML, Murray AB. 2008. Tidal marshes as disequilibrium landscapes? Lags between morphology and Holocene sea level change. Geophys Res Lett 35:L24401.

Kirwan ML, Walters DC, Reay WG, Carr JA. 2016. Sea level driven marsh expansion in a coupled model of marsh erosion and migration. Geophys Res Lett 43:4366–74.

Leonard LA, Luther ME. 1995. Flow hydrodynamics in tidal marsh canopies. Limnol Oceanogr 40:1474–84.

Marani M, D'Alpaos A, Lanzoni S, Carniello L, Rinaldo A. 2007. Biologically-controlled multiple equilibria of tidal landforms and the fate of the Venice lagoon. Geophys Res Lett 34:L11402.

Marani M, D'Alpaos A, Lanzoni S, Santalucia M. 2011. Understanding and predicting wave erosion of marsh edges. Geophys Res Lett 38:L21401.

Mariotti G, Carr J. 2014. Dual role of salt marsh retreat: long-term loss and short-term resilience. Water Resour Res 50:2963–74.

Mariotti G, Fagherazzi S. 2010. A numerical model for the coupled long-term evolution of salt marshes and tidal flats. J Geophys Res 115:F01004.

McKee KL. 2011. Biophysical controls on accretion and elevation change in Caribbean mangrove ecosystems. Estuar Coast Shelf Sci 91:475–83.

Morris JT, Sundareshwar PV, Nietch CT, Kjerfve B, Cahoon DR. 2002. Responses of coastal wetlands to rising sea level. Ecology 83:2869–77.

Mudd SM, Howell SM, Morris JT. 2009. Impact of dynamic feedbacks between sedimentation, sea-level rise, and biomass production on near surface marsh stratigraphy and carbon accumulation. Estuar Coast Shelf Sci 82:377–89.

Nicholls RJ, Hoozemans FMJ, Marchand M. 1999. Increasing flood risk and wetland losses due to global sea-level rise: regional and global analyses. Global Environ Change 9:S69–87.

Nyman JA, Delaune RD, Patrick WH Jr. 1990. Wetland soil formation in the rapidly subsiding Mississippi River Deltaic Plain: Mineral and organic matter relationships. Estuar Coast Shelf Sci 31:57–69.

Nyman JA, Walters RJ, Delaune RD, Patrick WH Jr. 2006. Marsh vertical accretion via vegetative growth. Estuar Coast Shelf Sci 69:370–80.

R Core Team. 2015. R: a language and environment for statistical computing. Vienna: R Foundation for Statistical Computing.

Rosen PS. 1977. Increasing shoreline erosion rates with decreasing tidal range in the Virginia Chesapeake Bay. Chesap Sci 18:383–6.

Shinkle KD, Dokka RK. 2007. Rates of vertical displacement at benchmarks in the Lower Mississippi Valley and the Northern Gulf Coast. Silver Spring: U.S. Department of Commerce, National Oceanic and Atmospheric Administration. p 147p.

Snedden GA, Swenson EM. 2012. Hydrologic index development and application to selected coastwide reference monitoring system sites and coastal wetlands planning, protection and restoration act projects. U.S. Geological Survey Open-File Report 2012–1122.

Steyer GD, Sasser CE, Visser JM, Swenson EM, Nyman JA, Raynie RC. 2003. A proposed coast-wide reference monitoring system for evaluating wetland restoration trajectories in Louisiana. Environ Monit Assess 81:107–17.

Temmerman S, Bouma TJ, Govers G, Wang ZB, De Vries MB, Herman PMJ. 2005. Impact of vegetation on flow routing and sedimentation patterns: Three-dimensional modeling for a tidal marsh. J Geophys Res 110:F04019.

Teal JM. 1962. Energy flow in the salt marsh ecosystem of Georgia. Ecology 43:614–24.

Turner RE, Swenson EM, Milan CS, Lee JM, Oswald TA. 2004. Below-ground biomass in healthy and impaired salt marshes. Ecol Res 19:29–35.

van de Koppel J, van der Wal D, Bakker JP, Herman PJM. 2005. Self-organization and vegetation collapse in salt-marsh ecosystems. Am Nat 165:E1–12.

Visser JM, Sasser CE. 1998. 1997 Coastal vegetation analysis. Baton Rouge, LA: Louisiana State University, Coastal Ecology Institute.